

Elastic Properties of Polymer-Decorated Membranes

Christin Hiergeist (*) and Reinhard Lipowsky

Max-Planck-Institut für Kolloid- und Grenzflächenforschung, Kantstr. 55, 14513 Teltow-Seehof, Germany

(Received 11 March 1996, revised 13 May 1996, accepted 13 June 1996)

PACS.05.40.+j – Fluctuation phenomena, random processes, and Brownian motion

PACS.36.20.-r – Macromolecules and polymer molecules

PACS.82.70.-y – Disperse systems

Abstract. — Polymers attached to one side of a fluid membrane induce a spontaneous curvature M_{sp} of the membrane and change its elastic constants. For an ideal polymer in the mushroom regime, we determine M_{sp} and the elastic constants κ and κ_G by an explicit calculation of the entropy gain of a polymer anchored onto a curved surface. For anchored polymers in the brush regime, a scaling picture is used to determine M_{sp} which increases monotonically with the coverage $\bar{\Gamma}$. For small and large $\bar{\Gamma}$, one has $M_{sp} \sim N^2 \bar{\Gamma}^{13/6}$ and $M_{sp} \sim N^{1/7} \bar{\Gamma}^{13/21}$, respectively. Both in the mushroom and in the brush regime, the polymers increase the bending rigidity, whereas the Gaussian bending rigidity is decreased.

1. Introduction

In biological systems, lipid bilayers are often “decorated” by a large number of macromolecules. The plasma membrane of animal cells, for instance, contains different membrane-spanning proteins. On the extracellular side, these proteins are coupled to a polymer brush called the glycocalix; on the intracellular side, to a network of filaments referred to as cytoskeleton [1]. Inspired by these biological structures, simplified model systems of polymers attached to lipid bilayers have been studied experimentally [2–4]. In these experiments it was observed that anchoring polymers to vesicles of fluid membranes induced dramatic changes in the vesicle shape [2]. Polymer-decorated vesicles also have an important application in medicine: coating vesicles with long flexible polymers increases their performance as drug delivery systems [5].

Polymers can be anchored onto membranes in several ways: by a lipid anchor, where a water-soluble polymer is covalently bound to a lipid molecule [4, 5] and by hydrophobic sidegroups of the polymer which protrude into the bilayer [2, 3]. Likewise, one could study block copolymers consisting of long hydrophilic blocks and short hydrophobic anchor parts. In the following, we will focus on the simplest polymer architecture which is provided by linear polymers with a single anchor at one end which may consist of a lipid molecule embedded in one monolayer or another hydrophobic segment spanning the whole bilayer.

Lipid bilayers exhibit several two-dimensional phases which differ in their elastic properties. Their most flexible state corresponds to the fluid phase and is governed by the bending energy

(*) Author for correspondence (e-mail: hiergeist@mpikg-teltow.mpg.de)

of the membrane. Contrary to a solid substrate, such a membrane can respond and adapt to the interactions with the polymers. We will consider anchored polymers which are effectively repelled from the membrane surface. The configurational entropy of the polymer chain depends on the shape of this surface and increases if the membrane bends away from it. Therefore, the anchored polymer tends to exert fluctuation or entropic forces onto the membrane and the bilayer attains a “spontaneous” curvature induced by the interactions with the anchored polymer [6].

In general, the polymers will be attached to both sides, *i.e.*, to both monolayers of the lipid bilayer. In practice, the anchor concentration in each monolayer can be varied by changing the polymer concentration in the adjacent solution and by changing the time over which the monolayer is exposed to this solution. The polymer coverage arising from this exposure of each monolayer depends both on the number of attached anchors and on the chain length of the anchored polymers. We will focus on the monodisperse case, *i.e.*, all polymers are assumed to have the same chain length.

If both monolayers exhibit a different polymer coverage, the decorated bilayer will be in an *asymmetric* state. In the limit of small curvatures, the polymer-induced curvature of such a state can be simply obtained by adding up the contributions arising from the two decorated monolayers. Therefore, it is sufficient to calculate the polymer-induced curvature for the extreme case in which all polymers are anchored to one side of the bilayer. This approach was used in reference [6] and will be extended below. Furthermore, the polymer-induced curvature of the bilayer vanishes only in the *completely symmetric* case for which the polymer coverage is identical on both monolayers. The latter situation has also been considered in reference [7].

In the low concentration regime, *i.e.*, for low polymer coverage or low anchor concentration, the anchored polymers form isolated mushrooms. For such a mushroom, the overall loss of entropy arising from the impenetrable membrane surface is only a few T (here and below, temperature is measured in energy units, *i.e.*, the Boltzmann constant k_B is contained in T). The anchoring energy ΔE_{an} , on the other hand, is typically of the order of many T : *e.g.*, for a lipid anchor with two hydrocarbon chains and n_c carbon atoms per chain, one has $\Delta E_{an} \simeq -1.7n_c T$ at room temperature $T = T_{room}$ [6]. Thus, in this mushroom regime, the free energy difference $\delta\mathcal{F}_{po}$ between the anchored and the freely suspended polymer state (which plays the role of an activation barrier) is large compared to T and the mean lifetime $t_{an} \sim \exp(|\delta\mathcal{F}_{po}|/T)$ of the anchored state is large compared to molecular time scales. In the following, we will focus on time scales which are smaller than t_{an} and will thus consider an ensemble in which the number of anchored polymers is fixed.

The mushroom regime extends up to the overlap coverage Γ_{ov} at which the membrane becomes completely covered by anchored polymers. For $\Gamma > \Gamma_{ov}$, one enters the semi-dilute brush regime in which the polymers experience an additional loss of entropy arising from the steric confinement by the neighbouring chains. Polymer brushes on flat and curved interfaces have been theoretically studied by scaling arguments [8–11] and by mean-field calculations [12,13]; a recent review is given in [14]. Below, we will extend the scaling approach and compare it with the corresponding mean-field calculation.

As the polymer coverage increases beyond the overlap coverage, the entropy loss arising from the steric confinement within the brush increases and the excess free energy $\delta\mathcal{F}_{po}$ of the anchored polymer relative to the freely suspended state decreases. As soon as $\delta\mathcal{F}_{po}$ becomes comparable to T , the lifetime t_{an} becomes comparable to molecular time scales and one may no longer ignore the exchange of polymers with the solution. The relation $\delta\mathcal{F}_{po} \simeq T$ defines a limiting polymer coverage Γ_{max} . It can be shown that Γ_{max} increases roughly linearly with the anchoring energy [6].

In general, the dissolved polymers may form dimers, trimers or more complex micelles.

Indeed, a dimer consisting of two polymers for which the two lipid anchors are in close contact should have a lower free energy than the two single polymers since the reduction in hydrophobic energy will be typically larger than the entropy loss of the polymer chains. Thus, in a two-component mixture of bilayer-forming lipids and polymers with lipid anchors, the formation of micelles may compete with the formation of bilayers as soon as the volume concentration of the polymers is sufficiently large. The phase diagrams arising from this competition has been recently studied both theoretically [15] and experimentally [16] ⁽¹⁾. In the present study, the volume concentration of the polymeric component is always taken to be so small that the lipids assemble into bilayers.

We first consider a single ideal polymer anchored onto a curved membrane segment, see Section 2. We calculate the excess free energy of the system relative to a flat configuration of the membrane in an expansion in the curvatures. To do this, we determine the entropy difference relative to a flat surface (i) of a polymer fixed with one end onto a sphere and (ii) of a polymer attached to a cylindrical surface. In both cases, the entropy difference is calculated up to second order in the reciprocal radius. In this way, we determine the effective elastic constants and the spontaneous curvature of the compound system. We find that the bending rigidity κ of the membrane is increased by the presence of the polymer, whereas the Gaussian bending rigidity κ_G is decreased.

In Section 3, we consider a membrane decorated by a polymer brush. Extending the scaling theory for polymer brushes on spherical and cylindrical surfaces, we deduce again the spontaneous mean curvature of the membrane and the effective bending rigidities. It turns out, that the spontaneous curvature exhibits different scaling behaviours for relatively low and relatively high polymer coverage. For small curvatures, the bending rigidity and the Gaussian bending rigidity are again increased and decreased, respectively.

2. Mushroom Regime

In this section we consider a single ideal polymer anchored at one end onto a curved membrane segment. The interaction between the polymer segments and the membrane is taken to be a pure hard wall interaction except for the anchor point.

In the following, we calculate the effective elastic constants and the spontaneous mean curvature of the decorated membrane. The polymer mushroom should influence the properties of the membrane on an area of the size of the cross-section of the polymer coil. The resulting effective elastic constants are therefore valid on a length scale comparable to the linear size of the polymer mushroom.

The curvature of the membrane segment is described by the mean curvature $M \equiv \frac{1}{2}(1/R_1 + 1/R_2)$ and the Gaussian curvature $G \equiv 1/R_1 R_2$, where R_1 and R_2 are the principal curvature radii. In the following, we analyze the excess entropy of the polymer anchored to a curved surface relative to the polymer anchored to a flat substrate

$$\Delta S_{\text{po}} \equiv S_{\text{po}}(M, G) - S_{\text{po}}(0, 0) \quad (1)$$

in an expansion in the curvatures. The size of the polymer mushroom is estimated by the mean end-to-end distance $R_{\text{po}} \approx a_{\text{po}} N^\nu$ of the polymer in solution, where N is the number of statistical segments of the chain and a_{po} the segment length, such that the full contour length of the polymer is equal to $a_{\text{po}} N$. For an ideal chain, the exponent $\nu = 1/2$.

⁽¹⁾ The aggregation into micelles has also been studied for aqueous solutions of polymers and surfactants, see, *e.g.* [17].

The excess entropy ΔS_{po} should be a function of the dimensionless variables $R_{\text{po}}M$ and R_{po}^2G . Expanding the excess entropy around the flat surface in the curvature radii up to second order yields [6]

$$\Delta S_{\text{po}}(M, G) = b_1 R_{\text{po}}M + b_2 (R_{\text{po}}M)^2 + b_3 R_{\text{po}}^2G + \dots \quad (2)$$

In general, the excess entropy also depends on the ratio $l_{\text{an}}/R_{\text{po}}$ where l_{an} represents the distance of the anchor segment to the membrane. Therefore, the expansion (2) should be valid in the scaling limit of small $l_{\text{an}}/R_{\text{po}}$.

In order to determine the coefficients b_1, b_2, b_3 of the expansion as given by (2) we are going to calculate $\Delta S_{\text{po}}(M, G)$ for spherical and cylindrical geometries, where the curvatures are $M = 1/R$, $G = 1/R^2$ and $M = 1/2R$, $G = 0$, respectively.

Consider the restricted partition function $Z_N(\mathbf{r}_{\text{an}}, \mathbf{r})$ of a polymer on a lattice with q nearest neighbours. The restricted partition function is the sum over all configurations starting at \mathbf{r}_{an} and ending at \mathbf{r} . In the continuum limit, the reduced weight

$$\mathcal{G}_N(\mathbf{r}_{\text{an}}, \mathbf{r}) \equiv Z_N(\mathbf{r}_{\text{an}}, \mathbf{r})/q^N \quad (3)$$

of an ideal polymer in zero external potential, obeys the diffusion equation

$$\left(\frac{\partial}{\partial N} - D \Delta_{\mathbf{r}} \right) \mathcal{G}_N(\mathbf{r}_{\text{an}}, \mathbf{r}) = 0 \quad (4)$$

together with the initial condition

$$\mathcal{G}_{N=0}(\mathbf{r}_{\text{an}}, \mathbf{r}) = \delta(\mathbf{r} - \mathbf{r}_{\text{an}}) \quad (5)$$

The diffusion coefficient is

$$D = a_{\text{po}}^2/q \quad (6)$$

[18]. The partition function \mathcal{Z} is then given by the integration of the restricted partition function $Z_N(\mathbf{r}_{\text{an}}, \mathbf{r})$ over all possible positions of the free end of the polymer

$$\mathcal{Z} = q^N W \quad (7)$$

with the total weight

$$W \equiv \int d\mathbf{r} \mathcal{G}_N(\mathbf{r}_{\text{an}}, \mathbf{r}) \quad (8)$$

Finally, the excess entropy $\Delta S_{\text{po}}(M, G)$ is given by $\Delta S_{\text{po}} = \ln(\mathcal{Z}/\mathcal{Z}_{\text{hs}})$, where \mathcal{Z}_{hs} is the partition function for a flat surface. In order to determine the coefficients in the expansion of the excess entropy (2), we calculate in the following (i) the partition function for a polymer anchored to a plane, (ii) the excess entropy of a polymer anchored to a sphere and (iii) the excess entropy of a polymer anchored to a cylinder.

2.1. POLYMER ANCHORED ON A PLANE. — To proceed, consider a polymer anchored at $\mathbf{r}_{\text{an}} = (l_{\text{an}}, 0, 0)$ above the plane $x = 0$. Then, the solution of equation (4) has the form [19]

$$\mathcal{G}_t(\mathbf{r}_{\text{an}}, \mathbf{r}) = (4\pi t)^{-3/2} \left\{ e^{-[(x-l_{\text{an}})^2 + y^2 + z^2]/4t} - e^{-[(x+l_{\text{an}})^2 + y^2 + z^2]/4t} \right\} \quad (9)$$

with $t \equiv DN$. Notice that the polymer size is $R_{\text{po}} = a_{\text{po}}N^{1/2} = \sqrt{qt}$. Integration over the possible positions \mathbf{r} of the second end point leads to [20]

$$W_{\text{hs}} = \text{erf}[\sqrt{q}l_{\text{an}}/(2R_{\text{po}})] \quad (10)$$

$$= \frac{\sqrt{q}l_{\text{an}}}{\sqrt{\pi}R_{\text{po}}} + \mathcal{O}((l_{\text{an}}/R_{\text{po}})^3) \quad , \quad (11)$$

where $\text{erf}[x]$ denotes the error function [21].

2.2. POLYMER ON A SPHERE. — Consider a polymer anchored at a distance l_{an} outside a sphere of radius R . The corresponding diffusion problem with a source at $\mathbf{r}_{an} \equiv (r_{an} = R + l_{an}, \theta_{an} = 0, \phi_{an} = 0)$ is solved by

$$\mathcal{G}_t(\mathbf{r}_{an}, \mathbf{r}) = \sum_{n=0}^{\infty} G_{t,n}(r_{an}, r) P_n(\cos \theta) \quad , \quad (12)$$

where $P_n(x)$ are Legendre polynomials [21]. The contribution corresponding to $n = 0$ is given by [19]

$$G_{t,0}(r_{an}, r) = \frac{1}{4\pi r_{an} r \sqrt{\pi t}} e^{-(l^2 + l_{an}^2)/4t} \sinh(l l_{an}/2t) \quad (13)$$

with $l \equiv r - R$

Integration over the position of the second end point yields

$$W = 4\pi \int_R^{\infty} dr r^2 G_{t,0}(r_{an}, r) \quad (14)$$

$$= \frac{l_{an}/R + \operatorname{erf}[l_{an}/(2\sqrt{t})]}{1 + l_{an}/R} \quad (15)$$

For the ratio of the partition functions, one finally obtains [6]

$$\mathcal{Z}/\mathcal{Z}_{hs} = \frac{1 + l_{an}/(R \operatorname{erf}[\sqrt{q}l_{an}/(2R_{po})])}{1 + l_{an}/R} \quad (16)$$

In the limit $l_{an}/R \ll 1$, this leads to

$$\mathcal{Z}/\mathcal{Z}_{hs} \approx 1 + \sqrt{\pi/q} R_{po}/R \quad (17)$$

Notice that there are no terms of order $(R_{po}/R)^2$.

For the spherical geometry, the excess entropy up to second order in the mean curvature $M = 1/R$ then reads

$$\Delta S_{po} = \sqrt{\pi/q} R_{po} M - (\pi/2q)(R_{po} M)^2 + \mathcal{O}((R_{po} M)^3) \quad (18)$$

This result is confirmed by an analogous calculation for a polymer anchored at a distance l_{an} inside a sphere. In this case, the reduced weight $\mathcal{G}_t(\mathbf{r}_{an}, \mathbf{r})$ is again of the form (12) with [19]

$$G_{t,0}(r_{an}, r) = \frac{1}{2\pi R^2 (r r_{an})^{1/2}} \sum_{\alpha} e^{-\alpha^2 t} \frac{J_{1/2}(\alpha r) J_{1/2}(\alpha r_{an})}{(J'_{1/2}(\alpha R))^2} \quad (19)$$

$$\text{and } \alpha = k\pi/R \quad , \quad k = 1, 2, \dots \quad (20)$$

Here, $J_{\nu}(x)$ are Bessel functions of the first kind [21]. Integration and expansion imply

$$\mathcal{Z}/\mathcal{Z}_{hs} \approx 1 - \sqrt{\pi/q} R_{po} R^{-1} \quad (21)$$

Again, there are no $\mathcal{O}((R_{po}/R)^2)$ terms. In the case of a spherical segment bending towards the polymer, the mean curvature is given by $M = -1/R$ and therefore (21) and (17) are equivalent.

2.3. POLYMER ON A CYLINDER. — In order to determine the coefficients in expansion (2) we have to calculate the excess entropy for another geometry. Therefore, we consider a polymer anchored outside an infinitely long cylinder of radius R . For an anchor point $\mathbf{r}_{\text{an}} \equiv (r_{\text{an}} = R + l_{\text{an}}, \theta_{\text{an}} = 0, z_{\text{an}} = 0)$ the reduced weight is given by

$$\mathcal{G}_t(\mathbf{r}_{\text{an}}, \mathbf{r}) = \frac{e^{-z^2/4t}}{2\sqrt{\pi t}} \sum_{n=-\infty}^{\infty} G_{t,n}(r_{\text{an}}, r) \cos(n\theta) \quad (22)$$

$$\text{with } G_{t,0}(r_{\text{an}}, r) = \frac{1}{2\pi} \int_0^{\infty} d\alpha \alpha e^{-\alpha^2 t} \frac{C_0(\alpha r, \alpha R) C_0(\alpha r_{\text{an}}, \alpha R)}{J_0^2(\alpha R) + Y_0^2(\alpha R)} \quad (23)$$

[19]. The function C_0 is defined as

$$C_0(x, y) \equiv J_0(x)Y_0(y) - Y_0(x)J_0(y) \quad , \quad (24)$$

where $J_\nu(x)$ and $Y_\nu(x)$ are Bessel functions of the first and second kind, respectively [21].

In order to calculate the total weight

$$W = 2\pi \int_R^{\infty} dr r G_{t,0}(r_{\text{an}}, r) \quad (25)$$

we first consider the limit $l_{\text{an}}/R \ll 1$ and perform then an expansion in \sqrt{t}/R . The details of this calculation are given in the Appendix. Finally, we obtain

$$W = \frac{l_{\text{an}}}{R} \left\{ \frac{1}{\sqrt{\pi}} \frac{R}{\sqrt{t}} + \frac{1}{2} - \frac{1}{4\sqrt{\pi}} \frac{\sqrt{t}}{R} + \mathcal{O}(t/R^2) \right\} \quad (26)$$

and for the ratio of the partition functions

$$\mathcal{Z}/\mathcal{Z}_{\text{hs}} = 1 + \frac{\sqrt{\pi}}{\sqrt{q}} R_{\text{po}} M - \frac{1}{q} (R_{\text{po}} M)^2 + \mathcal{O}((R_{\text{po}} M)^3) \quad (27)$$

The resulting excess entropy for the polymer anchored outside the cylinder is then

$$\Delta S_{\text{po}} = \frac{\sqrt{\pi}}{\sqrt{q}} R_{\text{po}} M - \left(\frac{\pi}{2q} + \frac{1}{q} \right) (R_{\text{po}} M)^2 + \mathcal{O}((R_{\text{po}} M)^3) \quad (28)$$

2.4. RESULTS. — Combining the excess entropy (18) and (28) for spheres with Gaussian curvature $G = M^2$ and cylinders with $G = 0$ with the general expansion (2) yields the coefficients

$$b_1 = +\sqrt{\frac{\pi}{q}} \quad (29)$$

$$b_2 = -\left(\frac{1}{q} + \frac{\pi}{2q} \right) \quad (30)$$

$$b_3 = +\frac{1}{q} \quad (31)$$

The excess free energy $\Delta \mathcal{F}_{\text{po}} = -T \Delta S_{\text{po}}$ of an ideal polymer anchored to a curved surface relative to a flat surface is therefore

$$\Delta \mathcal{F}_{\text{po}} = -\sqrt{\frac{\pi}{q}} T R_{\text{po}} M + \left(\frac{1}{q} + \frac{\pi}{2q} \right) T (R_{\text{po}} M)^2 - \frac{1}{q} T G R_{\text{po}}^2 + \mathcal{O}((R_{\text{po}}/R)^3) \quad (32)$$

This gain in free energy of the polymer is balanced by the bending energy of the membrane. The shape of the membrane should be influenced by the presence of the polymer on an area of the order of the cross-section of the polymer coil, *i.e.* an area $A = c_A R_{po}^2$, with c_A of order one. This implies a bending energy

$$\Delta \mathcal{E}_{me} = 2c_A \kappa (R_{po} M)^2 + c_A \kappa_G G R_{po}^2, \quad (33)$$

where κ is the bending rigidity and κ_G the bending modulus of the Gaussian curvature [22]. Finally, the total excess free energy $\Delta \mathcal{F} = \Delta \mathcal{F}_{po} + \Delta \mathcal{E}_{me}$ of the system reads

$$\begin{aligned} \Delta \mathcal{F} = & -b_1 T R_{po} M + 2c_A (\kappa/T - b_2/(2c_A)) T (R_{po} M)^2 \\ & + c_A (\kappa_G/T - b_3/c_A) T G R_{po}^2. \end{aligned} \quad (34)$$

Comparing the total excess free energy with the bending energy of the undecorated membrane segment (33) shows that the anchoring of a polymer changes the elastic constants to

$$\kappa_{eff} = \kappa + T \frac{1 + \pi/2}{2c_A q} \simeq \kappa + 0.21T \quad (35)$$

$$\kappa_{G,eff} = \kappa_G - T \frac{1}{c_A q} \simeq \kappa_G - 0.17T. \quad (36)$$

For the numerical values, we use $q = 2d = 6$ for a simple cubic lattice and $c_A = 1$. Notice that the corrections to the elastic constants are of opposite sign. For lipid bilayers, the bending rigidity is of the order of $10T - 20T$. The correction term arising from the polymer mushroom is therefore rather small.

The spontaneous mean curvature M_{sp} of the decorated membrane is given by the minimum of the total excess free energy at fixed Gaussian curvature,

$$\left. \frac{\partial \Delta \mathcal{F}}{\partial M} \right|_{M=M_{sp}} = 0 \quad (37)$$

Equation (34) therefore leads to the spontaneous mean curvature

$$M_{sp} = \frac{b_1}{4c_A (\kappa_{eff}/T) R_{po}} \quad (38)$$

$$= \sqrt{\pi} (4c_A \sqrt{q} (\kappa/T) + (2 + \pi)/\sqrt{q})^{-1} R_{po}^{-1}. \quad (39)$$

For $c_A = 1$ and $q = 6$, this leads to $M_{sp} \approx 0.18 (T/\kappa_{eff} R_{po})$. The parameter dependence

$$M_{sp} \sim T/\kappa_{eff} R_{po} \quad (40)$$

should also hold for a polymer under good solvent conditions as follows from scaling [6].

Using the effective elastic constants (35) and (36) and the spontaneous mean curvature (39), the total excess free energy can be written in the form

$$\Delta \mathcal{F}/A = -2\kappa_{eff} M_{sp}^2 + 2\kappa_{eff} (M - M_{sp})^2 + \kappa_{G,eff} G \quad (41)$$

The resulting effective constants (35) and (36) and the spontaneous mean curvature (39) are relevant on a length scale of the order of the polymer size R_{po} . On length scales which are large compared to R_{po} , the presence of the polymer mushrooms leads to inhomogeneous elastic constants of the membrane.

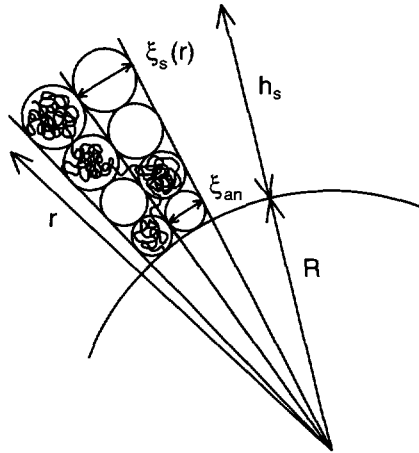


Fig. 1. — Scaling picture of a polymer brush on a sphere of radius R . The distance between the anchor points is ξ_{an} . The blob size scales as $\xi_s(r) = \xi_{an}r/R$ with the distance r from the sphere center. The brush height is denoted h_s .

3. Brush Regime

When the mean distance between the anchor molecules is smaller than the radius of the polymer coil, the polymers overlap and form a so-called polymer brush. As in the previous section, we focus on the spontaneous curvature and the elastic properties of an asymmetric membrane, *i.e.* a membrane covered by a polymer brush on one side. For the description of the polymer brush we extend the scaling picture for polymers grafted on spheres [10] and cylinders [11].

After presenting the scaling picture in which each chain is treated as a string of blobs (Sect. 3.1), we consider the spontaneous curvature of the decorated membrane (Sect. 3.2). We then analyze the limit of small curvatures (Sect. 3.3) and of large curvatures (Sect. 3.4). These two regimes correspond to relatively low and relatively high polymer coverage of the membrane, respectively. For both regimes, we determine the spontaneous curvature and the effective elastic constants of the decorated membrane. We compare our results with those derived using a mean-field theory for polymer brushes on curved surfaces [13].

The coverage is given by $\Gamma \equiv N/A_{po}$, where A_{po} is the area per anchored polymer which defines the grafting distance ξ_{an} via $A_{po} \equiv \xi_{an}^2$. The overlap coverage is $\Gamma_{ov} = N^{1-2\nu}/a_{po}^2$. The maximum value of the coverage is reached in the dense limit, $\Gamma_{de} = N/a_{po}^2$ (if one assumes that the anchoring energy is very large). It is then convenient to introduce the reduced coverage $\bar{\Gamma}$ defined by $\bar{\Gamma} \equiv \Gamma/\Gamma_{de} = (a_{po}/\xi_{an})^2$ which is the (dimensionless) number of polymers per unit area. Likewise, the anchor concentration is given by $(a_{an}/\xi_{an})^2$ where a_{an} is the lateral size of the lipid anchor.

In this section we are mainly interested in polymer brushes under good solvent conditions. Within the Flory approximation, the corresponding exponent ν has the numerical value $\nu \simeq 3/5$ which represents a rather good estimate.

3.1. SCALING PICTURE. — Within the blob picture for a polymer brush introduced by Alexander [8] and de Gennes [9] for a flat surface, one can describe a polymer brush on a sphere or a cylinder as consisting of concentric layers of blobs. In Figure 1 this picture is illustrated for a sphere. If X polymers are grafted onto the surface, then each layer contains X blobs of equal

size $\xi(r)$, where r is the distance from the center of the sphere or the axis of the cylinder. The size of the blobs in each layer increases with the distance from the grafting surface. The surface area of each such layer is given by $S(r) \approx X\xi(r)^2$.

For a sphere of radius R , $S(r) = 4\pi r^2$ and $X = 4\pi R^2/\xi_{\text{an}}^2$ which leads to the blob size

$$\xi_s(r) = \xi_{\text{an}} r/R \quad , \quad (42)$$

see also Figure 1. For a cylindrical surface of radius R , we have $S(r) \sim r$ and $X \sim R/\xi_{\text{an}}^2$ and therefore

$$\xi_c(r) = \xi_{\text{an}}(r/R)^{1/2} \quad (43)$$

Each blob contains $N_1(r) = (\xi(r)/a_{\text{po}})^{1/\nu}$ segments. The height of the brush $h(R)$ is implicitly given by

$$N = \int_R^{R+h} dr N_1(r)/\xi(r) \quad (44)$$

The free energy per polymer is proportional to the number of blobs,

$$\mathcal{F}_{\text{po}} = T \int_R^{R+h} dr 1/\xi(r) \quad (45)$$

Within this scaling picture, the height of a brush on a flat surface h_0 is given by

$$h_0 = N a_{\text{po}}^{1/\nu} \xi_{\text{an}}^{1-1/\nu} = N \bar{\Gamma}^{(1-\nu)/2\nu} a_{\text{po}} \quad (46)$$

The corresponding free energy reads

$$\mathcal{F}_{\text{po},0} = T \bar{\Gamma}^{1/2} h_0/a_{\text{po}} \quad (47)$$

In the following, we consider the gain in brush free energy per polymer on a curved surface relative to a flat surface at fixed polymer coverage, $\Delta\mathcal{F}_{\text{po}} \equiv \mathcal{F}_{\text{po}} - \mathcal{F}_{\text{po},0}$.

For the sphere, the scaling picture leads to the brush height

$$h_s(R) = R \left[\left(1 + \frac{h_0}{\nu R} \right)^\nu - 1 \right] \quad (48)$$

The free energy gain is given by

$$\Delta\mathcal{F}_{\text{po},s} = \mathcal{F}_{\text{po},0} f_s(h_0/R) \quad (49)$$

$$\text{with } f_s(x) = (\nu/x) \ln(1+x/\nu) - 1 \quad (50)$$

For the cylinder, one finds

$$h_c(R) = R \left[\left(1 + \frac{(1+\nu)h_0}{2\nu R} \right)^{2\nu/(1+\nu)} - 1 \right] \quad (51)$$

and

$$\Delta\mathcal{F}_{\text{po},c} = \mathcal{F}_{\text{po},0} f_c(h_0/2R) \quad (52)$$

$$\text{with } f_c(x) = \frac{1}{x} \left[\left(1 + \frac{1+\nu}{\nu} x \right)^{\nu/(1+\nu)} - 1 \right] - 1 \quad (53)$$

In principle, the expressions for N_1 , N , and \mathcal{F}_{po} could contain additional dimensionless coefficients. However, these coefficients will only affect the length scale h_0 and the energy scale $\mathcal{F}_{po,0}$ but will not change the relations (48-53).

We now want to argue that the same scaling picture may also be applied to a brush anchored to the *inside* of a sphere or cylinder (provided the innermost blob is larger than a_{po}). Within the blob picture, each chain anchored at the curved surface has essentially the same free energy as a chain which is confined within a truncated cone (each chain also undergoes a random walk parallel to the surface but this does not affect the arrangement of the blobs). The radius of this cone varies between $\xi(r = R) \equiv \xi_1$ at the membrane surface and $\xi(r = R + h) \equiv \xi_2$ at the other surface of the brush. For a brush which is anchored inside a sphere or cylinder, such a cone has $\xi_1 \equiv \xi_{an} > \xi_2 \equiv \xi(r = R - h)$ but the free energy arising from such a confinement may still be obtained within the blob picture. Alternatively, one may start from a brush which is anchored *outside* a sphere or cylinder and then cover it by a second membrane. If one now anchors the free ends of the polymers at this second surface and uproots the original anchors, one is left with a brush which is anchored to the inside of the second membrane surface. Since this process changes the chain conformation only in the boundary layers of blobs, the free energy of the brush should remain essentially unchanged. Indeed, it is not difficult to show that the free energy $\mathcal{F}_{po,s} = \mathcal{F}_{po,0} (f_s(h_0/R) + 1)$ with f_s as given by (50), for example, remains unchanged if one makes the replacement $M = 1/R \rightarrow M' = -1/(R + h)$ and $\xi_{an} \rightarrow \xi'_{an} = \xi_2 = \xi_{an}(1 + h/R)$.

Now consider a brush which is anchored inside a sphere or a cylinder. In order to apply the blob picture, the inner blob must be larger than the a_{po} . This condition implies $h_s(R) \lesssim R(1 - a_{po}/\xi_{an})$ and $h_c(R) \lesssim R(1 - (a_{po}/\xi_{an})^2)$. The corresponding free energies are given by (49) and (52), where R has to be replaced by $(-R)$. The above conditions imply that, for spherical and cylindrical surfaces, $1 - h_0/\nu R > 0$ and $1 - ((1 + \nu)h_0)/(2\nu R) > 0$, respectively.

Notice that the above scaling picture implies a segment concentration profile $c(r) \sim \xi(r)^{-4/3}$ for good solvent conditions. The radial decay of the concentration for a sphere and a cylinder is therefore given by $c_s(r) \sim r^{-4/3}$ and $c_c(r) \sim r^{-2/3}$, respectively. Numerical self-consistent field calculations [23] confirmed the $-4/3$ behaviour for the spherical geometry but led to a $c_c(r) \sim r^{-1/2}$ decay for the cylindrical case. The origin of the latter discrepancy remains to be clarified.

The free energy gain of the polymer brush $\Delta\mathcal{F}_{po}$ is again balanced by the bending energy of a membrane segment. Here, the corresponding membrane segment is of the size of the area per anchored polymer $A_{po} = a_{po}^2 \bar{\Gamma}^{-1}$. The bending energy then reads

$$\Delta\mathcal{E}_{me} = 2\kappa\bar{\Gamma}^{-1}(a_{po}M)^2 + \kappa_G\bar{\Gamma}^{-1}a_{po}^2G \quad (54)$$

up to second order in the principal curvatures. The next term is of order $(a_{me}M)^3$, where a_{me} represents the thickness of the bilayer. Thus, the above expression for $\Delta\mathcal{E}_{me}$ implicitly assumes that $M \ll 1/a_{me}$. For a phospholipid bilayer, one has $a_{me} \approx 4$ nm.

The total free energy change per polymer on the decorated membrane is now given by

$$\Delta\mathcal{F}_i = \Delta\mathcal{E}_{me}(M, G) + \Delta\mathcal{F}_{po,i}(R) \quad , \quad (55)$$

where $i = s$ and $i = c$ for spherical and cylindrical geometries, respectively.

3.2. SPONTANEOUS CURVATURE. — For a cylinder, the Gaussian curvature $G = 0$ and the mean curvature $M = 1/2R$. Thus, $\Delta\mathcal{F}_{po,c}$ depends only on M and the spontaneous mean curvature M_{sp} can be obtained by minimizing $\Delta\mathcal{F}_c$ with respect to M . This leads to the implicit equation

$$\frac{\partial f_c(x)}{\partial x} + 4(\kappa/T)N^{-3}\bar{\Gamma}^{-3/2\nu}x = 0 \quad (56)$$

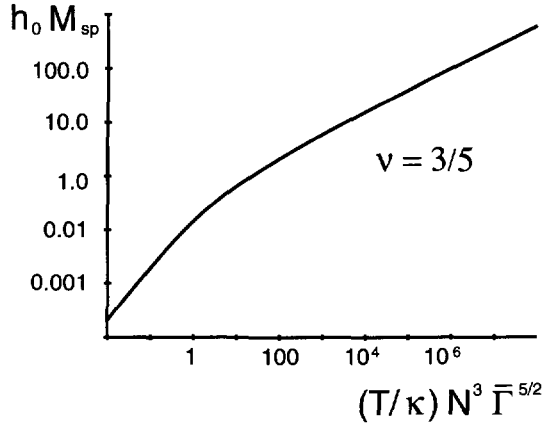


Fig. 2. — Spontaneous curvature M_{sp} of a membrane decorated by a polymer brush. The spontaneous curvature is rescaled by the height h_0 of the brush on a flat surface. The figure shows the solution of equation (56) under good solvent conditions ($\nu = 3/5$) as a function of the parameter combination $(T/\kappa)N^3\bar{\Gamma}^{5/2}$ where κ is the bending rigidity of the membrane, N the number of segments of the polymer, and $\bar{\Gamma}$ the reduced coverage.

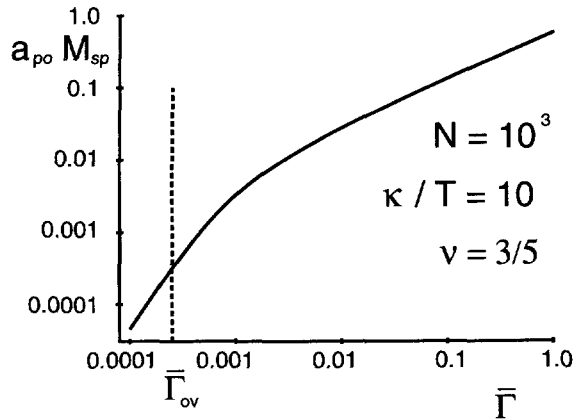


Fig. 3. — Spontaneous curvature $a_{po}M_{sp}$ as a function of the reduced coverage $\bar{\Gamma}$ under good solvent conditions and for fixed values of κ and N . a_{po} is the size of a polymer segment. The polymers are in the brush regime when the coverage is larger than the overlap coverage $\bar{\Gamma}_{ov}$. Notice that at high coverage, the spontaneous radius $1/M_{sp}$ becomes comparable to the length of a polymer segment.

for the spontaneous curvature

$$x \equiv h_0 M_{sp} \tag{57}$$

Figure 2 shows $h_0 M_{sp}$ as a function of $(T/\kappa)N^3\bar{\Gamma}^{3/2\nu}$ as obtained numerically from equation (56) for $\nu = 3/5$. Notice that at overlap coverage $\bar{\Gamma}_{ov} = N^{-2\nu}$, the parameter that controls equation (56) becomes $(T/\kappa)N^3\bar{\Gamma}_{ov}^{3/2\nu} = T/\kappa$. In Figure 3, $a_{po}M_{sp}$ is shown as a function of the reduced coverage for $N = 10^3$ and $\kappa = 10T$.

The free energy gain $\Delta\mathcal{F}_{\text{po},i}$ of the polymer depends on the radius only through the parameter $h_0/R \sim h_0M$. Thus, we will now study the limit of small and large h_0M by appropriate expansions of $\Delta\mathcal{F}_{\text{po},i}$.

Within an expansion for $h_0M \ll 1$ or $h_0M \gg 1$, the spontaneous curvature of the decorated membrane is determined consistently, if the resulting spontaneous curvature also satisfies $h_0M_{\text{sp}} \ll 1$ or $h_0M_{\text{sp}} \gg 1$. The regimes $h_0M_{\text{sp}} \ll 1$ and $h_0M_{\text{sp}} \gg 1$ correspond to low and high values of the parameter $(T/\kappa)N^3\bar{\Gamma}^{3/2\nu}$, respectively, as shown in Figure 2. The "crossover" value $h_0M_{\text{sp}} = 1$ is reached for $(T/\kappa)N^3\bar{\Gamma}^{3/2\nu} \simeq 20$ or the coverage

$$\bar{\Gamma}_* = c(\kappa/T)^{2/5} \bar{\Gamma}_{\text{ov}} \quad \text{for } \nu = 3/5 \quad (58)$$

with $c \simeq 3$. For lipid bilayers with $\kappa/T \simeq 10$, one has $\bar{\Gamma}_* \simeq 8\bar{\Gamma}_{\text{ov}}$. Therefore, the small curvature expansion ($h_0/R \ll 1$) is appropriate to determine M_{sp} for low polymer coverage of the order of $\bar{\Gamma}_{\text{ov}}$. On the other hand, the high curvature expansion ($h_0/R \gg 1$) corresponds to high coverage, $\bar{\Gamma}_{\text{ov}} \ll \bar{\Gamma} \lesssim 1$.

3.3. SMALL CURVATURE EXPANSION. — First, let us determine the spontaneous curvature and the effective elastic constants by expanding the free energy gain of the polymer brush $\Delta\mathcal{F}_{\text{po},i}$, as given by (49) and (52), up to second order in h_0/R , just as we did for the mushroom regime. For spherical and cylindrical geometries, this leads to

$$\Delta\mathcal{F}_{\text{po},s} = \mathcal{F}_{\text{po},0} \left[-\frac{1}{2\nu} \frac{h_0}{R} + \frac{1}{3\nu^2} \left(\frac{h_0}{R} \right)^2 + \mathcal{O}((h_0/R)^3) \right] \quad (59)$$

$$\text{and } \Delta\mathcal{F}_{\text{po},c} = \mathcal{F}_{\text{po},0} \left[-\frac{1}{2\nu} \frac{h_0}{2R} + \frac{\nu+2}{6\nu^2} \left(\frac{h_0}{2R} \right)^2 + \mathcal{O}((h_0/R)^3) \right], \quad (60)$$

respectively. Both expressions for the free energy gain, as given by (59) and (60), show a minimum as a function of $1/R$, whereas the original expressions (49) and (52) decrease monotonically. For the cylindrical case, the second-order expression for $\Delta\mathcal{F}_{\text{po},c}$ exhibits a minimum at $h_0/2R = 3\nu/(2\nu+4)$. Therefore, the expansion must break down for $h_0/2R \lesssim 3\nu/(2\nu+4)$.

The free energy gain (60) for a cylindrical surface leads to the spontaneous curvature

$$h_0M_{\text{sp}} = (1/2\nu) \left[4(\kappa/T)N^{-3}\bar{\Gamma}^{-3/2\nu} + (\nu+2)/(3\nu^2) \right]^{-1} \quad (61)$$

For $\bar{\Gamma} \gtrsim \bar{\Gamma}_{\text{ov}}$, $h_0M_{\text{sp}} \ll 1$ is indeed fulfilled. If one ignores the constant in the denominator, the spontaneous curvature is given by $a_{\text{po}}M_{\text{sp}} \simeq (8\nu)^{-1}(T/\kappa)N^2 \bar{\Gamma}^{(2+\nu)/2\nu}$ which scales as

$$a_{\text{po}}M_{\text{sp}} \sim N^2 \bar{\Gamma}^{13/6} \quad \text{for } \nu = 3/5 \quad (62)$$

Combining expression (59) for the sphere ($M = 1/R$, $G = M^2$) and expression (60) for the cylinder ($M = 1/2R$, $G = 0$) with the general expansion of the excess free energy up to second order in the curvatures,

$$\Delta\mathcal{F}_{\text{po}}(M, G) = \bar{b}_1 h_0 M + \bar{b}_2 (h_0 M)^2 + \bar{b}_3 h_0^2 G, \quad (63)$$

yields

$$\Delta\mathcal{F}_{\text{po}}(M, G) = \mathcal{F}_{\text{po},0} \left[-\frac{1}{2\nu} h_0 M + \frac{\nu+2}{6\nu^2} (h_0 M)^2 - \frac{1}{6\nu} h_0^2 G \right] \quad (64)$$

Comparing the total excess free energy of the compound system $\Delta\mathcal{F} = \Delta\mathcal{F}_{\text{po}} + \Delta\mathcal{E}_{\text{me}}$ to the bending energy of a bare membrane (54) leads to the effective bending constants

$$\kappa_{\text{eff}} = \kappa + \frac{\nu + 2}{12\nu^2} N^3 \bar{\Gamma}^{3/2\nu} T \quad (65)$$

$$\text{and } \kappa_{\text{G,eff}} = \kappa_{\text{G}} - \frac{1}{6\nu} N^3 \bar{\Gamma}^{3/2\nu} T \quad (66)$$

As in the case of isolated polymer mushrooms, see (35) and (36), the bending rigidity is increased by the anchored polymers whereas the Gaussian bending rigidity is decreased.

Using the effective bending rigidity (65), the spontaneous curvature (61) can be written in the form

$$a_{\text{po}} M_{\text{sp}} = (1/8\nu) N^2 \bar{\Gamma}^{(2+\nu)/2\nu} T / \kappa_{\text{eff}} \quad (67)$$

This equation should hold for $\bar{\Gamma} \gtrsim \bar{\Gamma}_{\text{ov}} = N^{-2\nu}$. At overlap coverage it leads to

$$a_{\text{po}} M_{\text{sp,ov}} = (1/8\nu) (a_{\text{po}} N^\nu)^{-1} (T / \kappa_{\text{eff}}) \quad (68)$$

At overlap coverage and under good solvent conditions ($\nu = 3/5$), the equations (65) and (66) yield $\kappa_{\text{eff}} = \kappa + (65/108)T$ and $\kappa_{\text{G,eff}} = \kappa_{\text{G}} - (5/18)T$ for the effective elastic constants. For a typical experimental situation ($N = 10^3$, $\kappa = 10T$, $a_{\text{po}} = 1/3 \text{ nm}$, $\nu = 3/5$), the relation (68) gives $M_{\text{sp,ov}} \simeq (10^3 \text{ nm})^{-1}$ as a rough estimate for the polymer induced spontaneous curvature at overlap coverage. On the other hand, the typical size of a large vesicle is $R_{\text{ve}} \simeq 10 \mu\text{m}$. The equilibrium shape of a vesicle is primarily determined by the reduced curvature $M_{\text{sp}} R_{\text{ve}}$, which in this case would be of the order of 10. Inspection of the phase diagram of the so-called spontaneous curvature model, which has been determined in references [24, 25], clearly shows that such a large value of $M_{\text{sp}} R_{\text{ve}}$ has a strong influence on the shape of the vesicle.

In order to compare these results with those of Section 2, we consider ideal chain behaviour ($\nu = 1/2$) at overlap coverage, leading to $\kappa_{\text{eff}} \approx \kappa + 0.8T$ and $\kappa_{\text{G,eff}} = \kappa_{\text{G}} - (1/3)T$. At overlap coverage, the brush consists of polymer mushrooms which touch each other, so that the results (35) and (36) can be applied. The appropriate area A of the membrane segment to be included in the energy balance is here the area per polymer $A = a_{\text{po}}^2 N^{2\nu} = R_{\text{po}}^2$. This implies $c_A = 1$, as used for the numerical values given in (35) and (36). In this limiting regime, the two approaches therefore lead to contributions of the same order. Likewise, at overlap concentration both approaches give an induced spontaneous curvature of the same form, see (38) and (68), the overall prefactor being again of the same order.

Milner and Witten [13] calculated the free energy gain of a polymer brush on a curved surface in an expansion in $1/R$ within a mean-field theory. Using their results for the case of moderately high coverage and not-too-good solvent, one obtains the spontaneous curvature $a_{\text{po}} M_{\text{sp}} \sim N^2 \bar{\Gamma}^2 T / \kappa$ and the effective elastic constants $\kappa_{\text{eff}} = \kappa + (9/64)(12/\pi^2)^{1/3} N^3 \bar{\Gamma}^{7/3} T$ and $\kappa_{\text{G,eff}} = \kappa_{\text{G}} - (3/35)(12/\pi^2)^{1/3} N^3 \bar{\Gamma}^{7/3} T$. Notice that the corrections to the elastic constants are of the same sign as those within the scaling theory. The dependence on $\bar{\Gamma}$, on the other hand, is slightly different: within the mean-field theory and the scaling theory one has $\kappa_{\text{eff}} - \kappa \sim \bar{\Gamma}^{7/3}$ and $\sim \bar{\Gamma}^{5/2}$, respectively, where the latter relation follows from (65) with $\nu = 3/5$. The small difference $\sim \bar{\Gamma}^{1/6}$ is due to correlation effects that are neglected in the mean-field theory.

Our results for membranes with polymers anchored to one side are easily extended to symmetrically decorated membranes. For one polymer brush anchored on each side of a cylindrical surface with reduced coverage $\bar{\Gamma}$, the free energy gain relative to the flat surface is given by

$$\Delta\mathcal{F}_{\text{po,c,2}} = + \frac{\nu + 2}{3\nu^2} \mathcal{F}_{\text{po,0}} (h_0 M)^2 \quad \text{for } h_0 M \ll 1 \quad (69)$$

as follows from (64). For a membrane decorated by polymers on both sides, the most favorable configuration is therefore the flat one. The polymer contribution to the effective bending rigidity is, in this case, twice the contribution of a single brush, $\kappa_{\text{eff},2} = \kappa + (\nu + 2)/(6\nu^2) N^3 \bar{\Gamma}^{3/2\nu} T$. Hristova and Needham [7] find for the symmetric case a contribution to the effective bending rigidity with the same parameter dependence using a somewhat different scaling approach.

3.4. LARGE CURVATURE. — With increasing polymer length and coverage of the membrane, the spontaneous curvature of the decorated membrane becomes larger, see Figure 3. We therefore consider now the high curvature regime with $h_0 M \gg 1$. On the other hand, we also assume that the bending energy given by (54) is still appropriate, implying $a_{\text{me}} M \ll 1$.

In the high curvature regime, the free energy of a polymer brush on a cylinder scales as

$$\mathcal{F}_{\text{po},c} \sim \mathcal{F}_{\text{po},0} (h_0 M)^{-1/(1+\nu)} \sim T N^{\nu/(1+\nu)} (aM)^{-1/(1+\nu)} \bar{\Gamma}^{1/(1+\nu)} \quad (70)$$

$$\sim T N^{3/8} \bar{\Gamma}^{5/8} M^{-5/8} \quad \text{for } \nu = 3/5 \quad (71)$$

[11]. Balancing with the bending energy leads to the spontaneous curvature

$$a_{\text{po}} M_{\text{sp}} \sim (T/\kappa)^{(1+\nu)/(3+2\nu)} N^{\nu/(3+2\nu)} \bar{\Gamma}^{(2+\nu)/(3+2\nu)} \quad (72)$$

$$\sim (T/\kappa)^{8/21} N^{1/7} \bar{\Gamma}^{13/21} \quad \text{for } \nu = 3/5 \quad (73)$$

This implies $h_0 M_{\text{sp}} \sim (\kappa/T)^{-8/21} N^{8/7} \bar{\Gamma}^{20/21}$ for $\nu = 3/5$. The free energy corresponding to this state scales as

$$\mathcal{F}_{\text{po},c}(M = M_{\text{sp}}) \sim T (\kappa/T)^{5/21} N^{2/7} \bar{\Gamma}^{5/21} \quad (74)$$

The range of parameters, however, that satisfies $h_0 M_{\text{sp}} \gg 1$ as well as $a_{\text{me}} M_{\text{sp}} = (a_{\text{me}}/a_{\text{po}}) \times a_{\text{po}} M_{\text{sp}} \ll 1$, is relatively small. For example, for poly(oxyethylene), which is rather flexible, the size a_{po} of the statistical segment of the polymers is of the order of the monomer size, $a_{\text{po}} \simeq 0.35$ nm. This corresponds to a situation where $a_{\text{me}}/a_{\text{po}} \simeq 12$.

For large curvature, the total excess free energy of the cylindrical system can be expanded around the spontaneous curvature M_{sp} following

$$\Delta \mathcal{F}_c = \Delta \mathcal{F}_c(M_{\text{sp}}) + \frac{1}{2} b (M - M_{\text{sp}})^2 + \dots \quad (75)$$

Comparing $\Delta \mathcal{F}_c$ with the general expression for the bending energy

$$\Delta \mathcal{E}_{\text{me}} = f_1(M_{\text{sp}}) + \frac{1}{2} \kappa_{\text{eff}} (2M - 2M_{\text{sp}})^2 A \quad (76)$$

where $A = A_{\text{po}}$ is the area involved, yields an effective bending rigidity for deformations around the spontaneous curvature. This effective bending rigidity is given by

$$\kappa_{\text{eff}} = \frac{1}{4A} \left. \frac{d^2 \Delta \mathcal{F}}{dM^2} \right|_{M=M_{\text{sp}}} \quad (77)$$

$$\approx (21/8) \kappa - c_1 \kappa^{8/7} N^{-3/7} \bar{\Gamma}^{-5/14} \quad \text{for } \nu = 3/5 \quad (78)$$

with $c_1 \simeq 0.5$. Notice that in the high curvature regime the effective elastic constants have only limited meaning, as the brush height and therefore the thickness of the “effective layer” is large compared to the radius.

Similar results for the spontaneous curvature and the effective bending rigidity are obtained by extending the mean-field theory [13] to large curvatures. The height of a brush on a cylinder

scales as $h_c \sim M^{-1/4} N^{3/4} \bar{\Gamma}^{1/4}$, as in the scaling picture, see equation (51). For the free energy one obtains

$$\mathcal{F}_{\text{po,c}}^{\text{MF}} \sim N^{1/2} \bar{\Gamma}^{3/2} M^{-1/2}, \quad (79)$$

leading to a spontaneous curvature

$$a_{\text{po}} M_{\text{sp}}^{\text{MF}} \sim (T/\kappa)^{2/5} N^{1/5} \bar{\Gamma} \quad (80)$$

and an effective bending rigidity

$$\kappa_{\text{eff}}^{\text{MF}} \approx (5/2)\kappa \quad (81)$$

4. Discussion

For an isolated, ideal polymer anchored onto a membrane, we calculated the free energy gain of a curved configuration relative to a flat membrane in an expansion up to second order in the curvatures. We found, that the effective bending rigidity κ_{eff} of the compound system is increased, whereas the effective Gaussian bending rigidity $\kappa_{\text{G,eff}}$ is decreased, relative to the corresponding elastic constants of the bare membrane. The corrections are however small compared to T . These effective elastic constants and the induced spontaneous curvature refer to an area of the order of the cross-section of the polymer coil. For large grafting distances, this leads to a membrane with inhomogeneous elastic properties.

We next studied a membrane covered by a polymer brush using a scaling approach. The resulting dependence of the spontaneous curvature on the coverage is shown in Figure 3. For relatively low polymer coverage, the induced spontaneous radius $1/M_{\text{sp}}$ is large compared to the height of the brush. In this regime, the effective bending rigidity is again increased and the effective Gaussian bending rigidity is again decreased by the presence of the polymers. The contribution scales in both cases as $N^3 \bar{\Gamma}^{5/2}$ for good solvent conditions. For relatively large polymer coverage, the spontaneous curvature scales as $M_{\text{sp}} \sim \kappa^{-8/21} N^{1/7} \bar{\Gamma}^{13/21}$. In this limit, the effective bending rigidity is renormalized to $\kappa_{\text{eff}} \approx (21/8)\kappa$.

In summary, we find that both in the mushroom and in the brush regime, the polymers induce a spontaneous curvature due to the entropy gain provided by the bending of the membrane. For the brush regime, the spontaneous curvature depends on the polymer length, the polymer coverage, and the solvent conditions. Therefore, the shape of a polymer-decorated vesicle should change, as one varies one of these parameters. As discussed after equation (68) the polymer induced spontaneous curvature will be of the order of $(10^3 \text{ nm})^{-1}$. Such a spontaneous curvature will affect the shape of a large vesicle (with a typical size of $10 \mu\text{m}$), as follows from the phase diagram in the spontaneous curvature model [24, 25].

In both regimes, the bending rigidity is increased and the Gaussian bending rigidity is decreased. In contrast, in the case of polymers *adsorbed* on membranes, the inverse result was found [26]. We have recently shown that the same distinction also applies to the spontaneous curvature: whereas an anchored but desorbed polymer exerts entropic forces which bend the membrane away from it as shown above, an adsorbed polymer pulls the membrane towards itself and induces a curvature of the opposite sign [27].

Finally, we want to mention that polymers anchored onto fluid membranes will not only change the elastic properties of the membrane itself, but will also influence the interaction between two membranes, brought in contact for instance by an external pressure.

Acknowledgments

We thank R. Bundschuh and A.V. Indrani for helpful and enjoyable discussions.

Appendix

Ideal Polymer on a Cylinder

The total weight W of an ideal polymer anchored outside a cylindrical surface at $\mathbf{r}_{\text{an}} \equiv (r_{\text{an}} = R + l_{\text{an}}, \theta_{\text{an}} = 0, z_{\text{an}} = 0)$ is obtained from

$$W = 2\pi \int_R^\infty dr r G_{t,0}(r_{\text{an}}, r) \quad (\text{A.1})$$

with $G_{t,0}(r_{\text{an}}, r)$ given by (23).

In the limit $l_{\text{an}}/R \ll 1$ this reduces to $W \approx (l_{\text{an}}/R)I$ with

$$I \equiv \int_1^\infty dr \int_0^\infty d\alpha r e^{-\alpha^2(t/R^2)} F(\alpha, r) \quad (\text{A.2})$$

$$\text{and } F(\alpha, r) \equiv \alpha^2 \frac{C_0(\alpha r, \alpha)(-J_1(\alpha)Y_0(\alpha) + Y_1(\alpha)J_0(\alpha))}{J_0^2(\alpha) + Y_0^2(\alpha)} \quad (\text{A.3})$$

with $C_0(x, y)$ as defined in (24). Notice that the order of the integrations in (A.2) cannot be changed, since the integral over r of the inner function diverges.

We are interested in an expansion of I for small

$$x \equiv \sqrt{t}/R = R_{\text{po}}/(\sqrt{q}R) \quad (\text{A.4})$$

For the inner integral in (A.2) this is obtained by an expansion of $F(\alpha, r)$ around $\alpha = \infty$,

$$\begin{aligned} F(\alpha, r) &= \alpha \left\{ \frac{2}{\pi} r^{-1/2} \sin((r-1)\alpha) \right\} + \left\{ \frac{1}{4\pi} r^{-3/2} \cos((r-1)\alpha)(r-1) \right\} \\ &+ \mathcal{O}(\alpha^{-1} \sin((r-1)\alpha)) \end{aligned} \quad (\text{A.5})$$

The α -integration then leads to

$$\begin{aligned} \int_0^\infty d\alpha F(\alpha, r) \exp(-\alpha^2 x^2) &= \frac{r-1}{2\sqrt{\pi r}} x^{-3} e^{-(r-1)^2/4x^2} + \frac{r-1}{8\sqrt{\pi r^3}} x^{-1} e^{-(r-1)^2/4x^2} \\ &+ \mathcal{O}(\text{erf}[-(r-1)/2x]) \end{aligned} \quad (\text{A.6})$$

Finally, this yields

$$I = \frac{1}{\sqrt{\pi}} x^{-1} + \frac{1}{2} + \mathcal{O}(x) \quad (\text{A.7})$$

For an expansion of ΔS_{po} up to second order in M , the coefficient of the third term in (A.7) is also required. This coefficient c_3 can be expressed as

$$c_3 = \frac{1}{2} \left[\frac{d^2}{dx^2}(xI) \right]_{x=0} \quad (\text{A.8})$$

Therefore, we consider

$$\frac{d^2}{dx^2}(xI) = -6x \int_1^\infty dr \int_0^\infty d\alpha r \alpha^2 e^{-\alpha^2 x^2} F(\alpha, r) + 4x^3 \int_1^\infty dr \int_0^\infty d\alpha r \alpha^4 e^{-\alpha^2 x^2} F(\alpha, r) \quad , \quad (\text{A.9})$$

where we again expand $F(\alpha, r)$ around $\alpha = \infty$. The α -integration leads again to integrals of the type $\int dr f(r, x) e^{-r^2/4x^2}$, which in turn can be evaluated for small x expanding $f(r, x)$ for small r . This implies

$$\frac{d^2}{dx^2}(xI) = -\frac{1}{2\sqrt{\pi}} + \frac{3}{2}x + \mathcal{O}(x^2) \quad (\text{A.10})$$

and

$$c_3 = -\frac{1}{4\sqrt{\pi}} \quad (\text{A.11})$$

Together with (A.7) we therefore obtain

$$W = \frac{l_{\text{an}}}{R} \left\{ \frac{1}{\sqrt{\pi}} \frac{R}{\sqrt{t}} + \frac{1}{2} - \frac{1}{4\sqrt{\pi}} \frac{\sqrt{t}}{R} + \mathcal{O}(t/R^2) \right\} \quad (\text{A.12})$$

References

- [1] "Structure and dynamics of membranes", Vol. 1 of Handbook of biological physics, R. Lipowsky and E. Sackmann Eds. (Elsevier, Amsterdam, 1995).
- [2] Decher G., Kuchinka E., Ringsdorf H., Venzmer J., Bitter-Suermann D. and Weisgerber C., *Angew. Makromol. Chem.* **166/167** (1989) 71.
- [3] Simon J., Kühner M., Ringsdorf H. and Sackmann E., *Chem. Phys. Lipids* **76** (1995) 241.
- [4] Blume G. and Cevc G., *Biochim. Biophys. Acta* **1029** (1990) 91.
- [5] Lasic D., *Angew. Chem. Int. Ed. Engl.* **33** (1994) 1685.
- [6] Lipowsky R., *Europhys. Lett.* **30** (1995) 197.
- [7] Hristova K. and Needham D., *J. Colloid Interface Sci.* **168** (1994) 302; *Liq. Cryst.* **18** (1995) 423.
- [8] Alexander S., *J. Phys. France* **38** (1977) 983.
- [9] de Gennes P.-G., *J. Chem. Phys.* **72** (1980) 4756.
- [10] Daoud M. and Cotton J., *J. Phys. France* **43** (1982) 531.
- [11] Zhulina Y.B. and Birshstein T.M., *Polymer Sci. USSR* **27** (1985) 570.
- [12] Cantor R., *Macromolecules* **14** (1981) 1186.
- [13] Milner S. and Witten T., *J. Phys. France* **49** (1988) 1951.
- [14] Halperin A., Tirrell M. and Lodge T., *Adv. Polym. Sci.* **100** (1992) 31.
- [15] Hristova K. and Needham D., *Macromolecules* **28** (1995) 91.
- [16] Kenworthy A., Simon S. and McIntosh T., *Biophys. J.* **68** (1995) 1903.
- [17] Lindman B. and Thalberg K., in Interactions of surfactant with polymers and proteins, E. Goddard and K. Ananthapadmanabhan Eds. (CRC Press, Boca Raton, 1993).
- [18] de Gennes P.-G., Scaling concepts in polymer physics (Cornell University Press, Ithaca, 1979).
- [19] Carslaw H. and Jaeger J., Conduction of heat in solids (Clarendon Press, Oxford, 1959).
- [20] Eisenriegler E., Polymers near Surfaces (World Scientific, Singapore, 1993).
- [21] Handbook of mathematical functions, M. Abramowitz and I. Stegun Eds. (Dover Publications, Inc., New York, 1965).
- [22] Helfrich W., *Z. Naturforsch.* **28c** (1973) 693.
- [23] Dan N. and Tirell M., *Macromolecules* **25** (1992) 2890.
- [24] Seifert U., Berndt K. and Lipowsky R., *Phys. Rev. A* **44** (1991) 1182.
- [25] Miao L., Seifert U., Wortis M. and Döbereiner H.-G., *Phys. Rev. E* **49** (1994) 5389.
- [26] Brooks J., Marques C. and Cates M., *J. Phys. II France* **1** (1991) 673.
- [27] Hiergeist C., Indrani A.V. and Lipowsky R. (to be published).